Constraints equations, a numerical method to connect a multibody model with a finite element model when a planar mechanism slides with a friction on a beam

Krzysztof Lipiński

Faculty of Mechanical Engineering, Gdańsk University of Technology
ul. Narutowicza 11/12, 80-233 Gdańsk, Poland
e-mail: klipinsk@pg.gda.pl

Abstract

In the paper, dynamics of a hybrid system composed of a multibody model and a deformable beam structure is considered. The multibody system is in a sliding contact with the beam and the friction forces are present at the contact point. To express the contact, constraint equations are introduced. The paper zoom is set to the constraint equations. At present, the considered case is restricted to the planar case and to the multibody systems composed of rigid bodies. For the multibody system, joint relative displacements are considered as the generalised coordinates. Significant displacements as well as the nonlinear effects (as Coriolis accelerations) are considered. For the finite element, nodes displacements are considered as the coordinates. Shape functions are used to express displacements and velocities. Referring to the classical joint partitioning method [6], the dependent and the independent coordinates are selected. A modified version of the partitioning method is proposed in the paper to account the friction force (Lagrange multiplier dependent), as well as to eliminate the non-necessary zero operations present in the classical algorithm. Finally, an exemplary system and its time simulations are presented.

Keywords: computational mechanics, multibody system, finite elements, constraint equations, coordinate partitioning, friction

1. Introduction

In the paper, a contact between a multibody model and an elastic, deformable structure is considered. The multibody system is in a sliding contact with the structure and the friction force is present at the contact point. The classical Coulomb friction hypothesis is introduced. The paper concentrates on the slip phase only. To model the stick phase, an essentially different numerical model is necessary. To model it, an additional lateral constrain has to be introduced. According to it, the stick phase is not included in the current model.

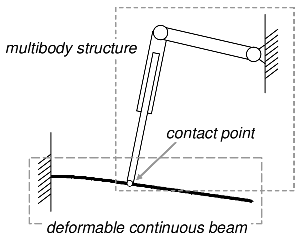

Figure 1: Elements of the considered system

Relatively bibliography is seldom. However, a lot of practical applications is associated with the proposed situation. A wheel rail contact is an example [1], where the rail was considered as a deformable element. The train's energy supply system composed of pantograph\contact line\catenary is the other example [2, 3]. In the cited cases, an elastic contact is proposed to model the contact, i.e. a damper and a spring are introduced between the multibody and the elastic systems. As pointed in some previous works of the author [7, 8], the constraint equations look as an interesting alternative, used to model the contact, but the friction forces was not considered in the previous presentations, yet.

To prepare the model, the classical multibody modelling, as well as the classical finite element modelling, is considered in the paper. The multibody system is composed of rigid-body bodies. One-degree of freedom joints are used to connect them. Joints' relative displacements are taken as the sub-system's generalised coordinates. Their deformations (i.e. the joint displacements) are considered as significant (i.e. significant changes of the body orientations are considered in the model). Then equations of kinematics, as well as equations of dynamics, are deliberated. A method proposed in [4, 5] is employed. The modelled multibody system forms a single kinematic chain structure composed of *n* bodies, i.e. a method devoted to three-like systems should be sufficient to model the system. An $n \times n$ square mass matrix and an *n*-dimensional vector (a column matrix) of general forces can be obtained for the system. The last vector collects influences of all the nonlinear effects as: the centrifugal accelerations or Coriolis accelerations.

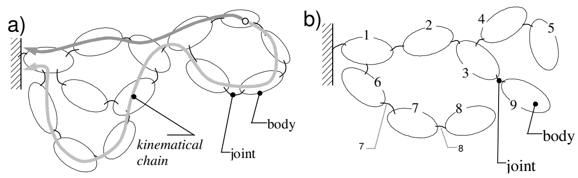

Figure 2: Exemplary multibody systems: closed kinematical chains (a); a tree structure with a numbering proposition (b)

When the focus is set on the considered finite elements model, it is considered as composed of short deformable elements. A set of points (nodes) is selected for each of the deformable element. Their displacements are taken as the sub system generalised coordinates. For the rest of the points, nodes displacements and user defined shape functions are necessary to determine their shifts. As the elastic structure corresponds to some stationary located sub system, its drift motion is absent, and the nodes' displacements are small. To obtain the dynamics equations a method proposed in [7-2] is employed. Resulting equations are linear in respect to the node displacements, velocities and accelerations. According to it, the mass, dissipation and stiffness matrices can be calculated.

In the considered model, the dynamics of the sub-systems is expressed with the classical methods. As an extension, the present paper focuses on the constraint equations. A set of scleronomic, holonomic constraints is proposed. In the constraints, a rigid contact is considered, i.e. the contact is restricted to a single contact point. The point can slides along the elastic element. By contrast to the author's previously presented cases [7, 8], a slip with a friction is introduced between the sliding elements.

An additional extension is present in the coordinate partitioning. As in the classical partitioning method [6], the generalised coordinates of the initial unconstrained system have to be partitioned on dependent and independent variables. However a significant modification is necessary to fit the method to the system compost of multibody and finite elements model, and to the case of when applied friction forces depend explicitly on the Lagrange multipliers. Details of the proposed elimination method form a significant part of the paper.

To verify the proposed equations, an exemplary numerical model is proposed. A planar manipulator and a planar continuous beam are considered. Time simulations of its behaviour are performed and presented.

To deal with the introduced problems, the paper is divided onto ten sections. In the subsequent, i.e. in the one after the introduction, fundaments of the used multibody formalism are presented. Equations of the three-like structures are presented. The third section presents fundaments of used finite elements formalism. General idea of the method is presented, as well as exemplary matrices for the beam element. Sections four to eight form the main part of the paper. Constraint equations of the punctual contact between the multibody system and the finite elements model are presented in section four. The fifth section presents the velocity analysis at the contact point (slip formulas). Proper determination of its direction is an essential element of the model. The sixth section describes consequences of the frictionless contact. They are introduced as some reference for the future divagations. In paragraph seven, generalized forces associated to the friction forces are determined. In the next section, the dynamics equations are presented for the system with the friction forces. Proposed modified version of the partitioning method is described in the section, too. Section nine presents an exemplary reference model. The introduced model is used for the numerical tests. Results of the performed tests are presented in the section, too. The last section summarise the main conclusions.

2. Multibody model

In the section fundaments of the used algorithm are presented. The used algorithm is based on the standards presented in [4, 5, 7, 8]. The introduced multibody system (*MbS*) is defined as composed of inertial, rigid bodies. Its bodies can change their relative position and orientations. All the potential displacements are restricted to *connections*, where the last are supposed as deformable and massless elements. In general, connections refer to some multi degrees-of-freedom elements. However, when restricted to the one-degree-of-freedom, prismatic or revolute type, name *joints* is introduced to distinguish the difference. Joints are sufficient to describe the *MbS*, since each of the multi-degrees-of-freedom connections can be modelled as an ordered sequence of joints, massless bodies and constraints is some of the cases. With the presented introduction, the analysed *MbS*'s structure is treated as a sequence of bodies interconnected by joints. A term *kinematical chain* (*kCh*) is used to refer to such sequences. In general, different strategies can be proposed to select the *system's generalised coordinates* (*gSC*) [11]. In the present case, the relative joint displacements (joint coordinates) are considered.

For a generic *body N^o i* (denoted as B^i), the most fundamental is the *reference kCh*, i.e. a *kCh* between B^i with the reference body (numbered as 0). For simplicity, the *kCh* is denoted as ${}^0kCh^i$. In some of the cases, the contents of the ${}^0kCh^i$ may be determined in a unique way. In each of such cases, the *kCh* is called as an *open kCh*. Otherwise, a *closed kCh* is present in the system (Fig. 2b). Moreover if none on the *MbS*'s *kCh* is of the closed type, the *MbS* is called as a *tree structure* (Fig. 2a). Its alternative is called as a *closed MbS* (Fig. 2b).

The introduced definition states that, when tree structures are considered, the succession order is unique. Thus, the body numbering can be introduced for such systems. It coincides with the succession order observed in the reference *kCh*s. In its detailed description, when a body of ${}^0kCh^i$ is considered, its number has to be lower or at least equal to *i*. Next, a redefinition of a classical $j<i$ symbol is useful. It denotes the B^j as an element of ${}^0kCh^i$. Then, i^+ symbol denotes the complete set composed of bodies that succeed the B^i directly. Per analogy, i^- symbol denotes the B^i direct predecessor. Finally, for the joint numbering, the joint between B^i and B^{i-} is numbered as *i* (for simplicity, this joint is denoted as J^i).

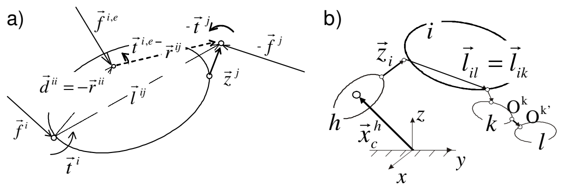

Figure 3: Geometry of the *MbS*: geometrical dimensions and interactions acting on B^i (a); geometrical dimensions of the *MbS* (b)

When a vector fixed to B^i is considered, its coordinates are constant, when express in the body fixed system. To express them in the reference body fixed system, orientation matrices, $\boldsymbol{T}^i$, are necessary. They are coordinates dependent and are calculated as some ordered products of the relative orientation matrices, $\boldsymbol{R}^j$, present in the ${}^0kCh^i$. Similar reflections can be formulated for the $\vec{x}^i$ vector (it locates the mass centre with respect to the origin of the reference system). The introduced vector is a sum of distances present in the ${}^0kCh^i$. Together with the symbols presented in Fig. 3, ones can obtain [4, 5, 7, 8]

$$\boldsymbol{T}^i = \prod_{j:j\le i} \boldsymbol{R}^j \qquad ; \qquad \vec{x}^i = \sum_{j:j\le i} \left(\vec{z}^j + \vec{d}^{ji} \right) \tag{1}$$

When Eqs (1) are differentiated, it leads to [4, 5, 7, 8]

$$\vec{\omega}^i = \sum_{k:k\le i} \dot{\varphi}^k \cdot \vec{e}^k \quad ; \quad \dot{\vec{x}}^i = \sum_{k:k\le i} (\dot{p}^k \cdot \vec{a}^k + \vec{\omega}^k \times \vec{l}^{ki}) \tag{2ab}$$

$$\dot{\vec{\omega}}^i = \sum_{k:k\le i} (\ddot{\varphi}^k \cdot \vec{e}^k + \dot{\varphi}^k \cdot \vec{\omega}^k \times \vec{e}^k) \tag{2c}$$

$$\ddot{\vec{x}}^i = \sum_{k:k\le i} (\ddot{p}^k \cdot \vec{a}^k + \dot{\vec{\omega}}^k \times \vec{l}^{ki} + 2\,\dot{p}^k \cdot \vec{\omega}^k \times \vec{a}^k + \vec{\omega}^k \times \vec{\omega}^k \times \vec{l}^{ki}) \tag{2d}$$

where: p^j – magnitude of the translational displacement; $\vec{a}^j$ – translational *mobility unit vector*; φ^j – rotation angle in the rotational joint; $\vec{e}^j$ – rotational mobility unit vector (collinear to joint axis of the rotation).

Let us point an aspect of the introduced definition. The $\vec{a}^j$ vector is zero long for rotational joints, as well as the $\vec{e}^j$ vector is zero for translational joints, too. Next, when zoom is set on the obtained equations, a matrix form can be used to express them. It leads to [7, 8]:

$$\vec{\omega}^i = \vec{\boldsymbol{A}}^{2,i} \cdot \dot{\boldsymbol{q}}^b \quad ; \quad \dot{\vec{x}}^i = \vec{\boldsymbol{A}}^{1,i} \cdot \dot{\boldsymbol{q}}^b \; ; \tag{3ab}$$

$$\dot{\vec{\omega}}^i = \vec{\boldsymbol{A}}^{2,i} \cdot \ddot{\boldsymbol{q}}^b + \dot{\vec{\omega}}^{i,R} \; ; \quad \ddot{\vec{x}}^i = \vec{\boldsymbol{A}}^{1,i} \cdot \ddot{\boldsymbol{q}}^b + \ddot{\vec{x}}^{i,R} \tag{3cd}$$

where: $\boldsymbol{q}^b$ – column matrix of *gSC*; $\vec{\boldsymbol{A}}^{1,i}$, $\vec{\boldsymbol{A}}^{2,i}$ – row matrices of vectors[1]; $\ddot{\vec{x}}^{i,R}$, $\dot{\vec{\omega}}^{i,R}$ – acceleration's "remainders" independent of joint accelerations.

To obtain the *dynamic equations* (*DE*), free body diagrams are composed for all bodies of the system. To obtain it, the connecting point between the B^i and the J^i are cut and replaced by the joint interactions. Next, the Newton/Euler dynamics equations are used for the bodies. Obtained *DE* may be written as [4, 5, 7, 8]:

$$m^i \cdot \ddot{\vec{x}}^i = \vec{f}_i + \vec{f}_i^{\,e} - \sum_{j\in i^+} \vec{f}_j^{\,i} \quad ; \tag{4a}$$

$$\vec{\omega}^i \times (\bar{\bar{I}}^i \cdot \vec{\omega}^i) + \bar{\bar{I}}^i \cdot \dot{\vec{\omega}}^i = \vec{t}_{iC} + \vec{r}^{\,ii} \times \vec{f}_i + \vec{t}_{iC}^{\,e} - \sum_{j\in i^+} \vec{t}_{jC}^{\,i} - \sum_{j\in i^+} \vec{r}^{\,ij} \times \vec{f}_j^{\,i}, \tag{4b}$$

where: m^i – mass of B^i; $\bar{\bar{I}}^i$ – its tensor of moments of inertia about the mass centre; $\vec{f}^{\,i}$, $\vec{t}^{\,i}$ – force and torque at the B^i/J^i point; $\vec{f}_i^{\,e}$ – net external at B^i; $\vec{t}_{iC}^{\,e}$ – net external torque at B^i calculated about the mass centre.

The *DE* (4) are combined with the kinematics (3) to [7, 8]:

$$\vec{\boldsymbol{B}}^{1,i} \cdot \ddot{\boldsymbol{q}}^b + m^i \cdot \ddot{\vec{x}}^{i,R} = \vec{f}_i + \vec{f}_i^{\,e} - \sum_{j\in i^+} \vec{f}_j^{\,i} \quad ; \tag{5a}$$

$$\begin{aligned} &\vec{\boldsymbol{B}}^{2,i} \cdot \ddot{\boldsymbol{q}}^b + \vec{\omega}^i \times \left(\bar{\bar{I}}^i \cdot \vec{\omega}^i\right) + \bar{\bar{I}}^i \cdot \dot{\vec{\omega}}^{i,R} = \\ &\qquad = \vec{t}_{iC} + \vec{r}^{\,ii} \times \vec{f}_i + \vec{t}_{iC}^{\,e} - \sum_{j\in i^+} \vec{t}_{jC}^{\,i} - \sum_{j\in i^+} \vec{r}^{\,ij} \times \vec{f}_j^{\,i} \; , \end{aligned} \tag{5b}$$

where: $\vec{\boldsymbol{B}}^{1,i} = m^i \vec{\boldsymbol{A}}^{1,i}$, $\vec{\boldsymbol{B}}^{2,i} = \bar{\bar{I}}^i \cdot \vec{\boldsymbol{A}}^{2,i}$ – matrices of coefficients.

The first summands at (5), are not the lonely terms dependent on the joint accelerations. The successors' forces and torques depend on them, too. To eliminate them, the backward elimination is applied, i.e. the force evaluation starts from the system final bodies. With the algorithm used iteratively (till the J^i is reached), the searched interactions can be written as [7, 8]

$$\vec{f}^{\,i} = \vec{\boldsymbol{C}}^{1,i} \cdot \ddot{\boldsymbol{q}}^b + \vec{\boldsymbol{D}}^{1,i} + \vec{\boldsymbol{E}}^{1,i} \quad ; \quad \vec{t}^{\,i} = \vec{\boldsymbol{C}}^{2,i} \cdot \ddot{\boldsymbol{q}}^b + \vec{\boldsymbol{D}}^{2,i} + \vec{\boldsymbol{E}}^{2,i} \; , \tag{6a}$$

where:

$$\begin{aligned} &\vec{\boldsymbol{C}}^{1,i} = \sum_{l:i\le l} \vec{\boldsymbol{B}}^{1,l} \; ; \\ &\vec{\boldsymbol{C}}^{2,i} = \sum_{l:i\le l} \left[\vec{\boldsymbol{B}}^{2,l} + \left(\sum_{k:i\le k\le l} \vec{l}^{\,kl} \right) \times \vec{\boldsymbol{B}}^{1,l} \right]; \\ &\vec{\boldsymbol{D}}^{1,i} = \sum_{l:i\le l} m^l \cdot \ddot{\vec{x}}^{l,R} \; ; \\ &\vec{\boldsymbol{D}}^{2,i} = \sum_{l:i\le l} \left[\vec{\omega}^l \times \left(\bar{\bar{I}}^l \cdot \vec{\omega}^l \right) + \bar{\bar{I}}^l \cdot \dot{\vec{\omega}}^{l,R} + m^l \cdot \left(\sum_{k:l\le k\le l} \vec{l}^{\,kl} \right) \times \ddot{\vec{x}}^{l,R} \right]; \\ &\vec{\boldsymbol{E}}^{1,i} = -\sum_{l:j\le l} \vec{f}^{\,l,e} \; ; \\ &\vec{\boldsymbol{E}}^{2,i} = -\sum_{l:i\le l} \vec{t}^{\,l,e} - \sum_{l:i\le l} \left(\sum_{k:i\le k\le l} \vec{l}^{\,kl} \right) \times \vec{f}^{\,l,e} \; . \end{aligned} \tag{6b}$$

To obtain their independent component, interactions from (6a) are projected into mobility vectors ($\vec{a}^{\,i}$ and $\vec{e}^{\,i}$ respectively). After it, the *DE*s are turned into the following from

$$\boldsymbol{M}^b(\boldsymbol{q}^b) \cdot \ddot{\boldsymbol{q}}^b + \boldsymbol{F}^b(\dot{\boldsymbol{q}}^b, \boldsymbol{q}^b, \boldsymbol{f}_e, \boldsymbol{t}_e, t) = \boldsymbol{Q}^b \; , \tag{7a}$$

where: $\boldsymbol{Q}^b$ – active action at the system joints,

$$\boldsymbol{M}^b = \vec{a}^{\,i} \circ \vec{\boldsymbol{C}}^{1,i} + \vec{e}^{\,i} \circ \vec{\boldsymbol{C}}^{2,i} \; ; \tag{7b}$$

$$\boldsymbol{F}^b = \vec{a}^{\,i} \circ (\vec{\boldsymbol{D}}^{1,i} + \vec{\boldsymbol{E}}^{1,i}) + \vec{e}^{\,i} \circ (\vec{\boldsymbol{D}}^{2,i} + \vec{\boldsymbol{E}}^{2,i}) \; ; \tag{7c}$$

3. Finite element model

As in the previous section fundaments of the used standard algorithm are presented according to the standards presented in [9, 10]. In the model, displacements at a finite number of nodes' are treated as s system's generalized coordinates. In the general case, each of the nodes has six degrees of freedom (i.e. three translational and three rotational). In particular cases, the dedicated number of degrees is lower. For planar beam element, two degrees of freedom are sufficient (vertical and rotational).

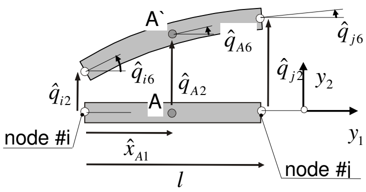

Figure 4: Details of the beam finite element

To describe the system parameters, global coordinate system is fixed to the reference body, as well as some local systems fixed to the initial, non-deformed elements. When the element deformations are described in the local coordinate system, to underline it, symbol ^ is introduced above of its parameter name. Within the adopted convention, it is supposed that vertical displacements are performed along $\hat{y}_2$ axis, and rotations are made about $\hat{y}_3$. Thus, when the element nodes are numbered as *i* and *j*, the element coordinates are [9, 10]

$$\hat{\boldsymbol{q}}_{\boldsymbol{e}} = col(\hat{q}_{i2}, \hat{q}_{i6}, \hat{q}_{j2}, \hat{q}_{j6}) \; , \tag{8}$$

where: $\hat{q}_{i2}, \hat{q}_{j2}$ – beam translations along y_2 (Fig. 4b), $\hat{q}_{i6}, \hat{q}_{j6}$ – beam rotations about y_3 (Fig. 4b).

In the considered case, system loads could be attached in the system's nodes, only. According to it, the load vector is:

$$\hat{\boldsymbol{P}}_{\boldsymbol{e}} = col(\hat{P}_{i2}, \hat{P}_{i6}, \hat{P}_{j2}, \hat{P}_{j6}) \; , \tag{9}$$

where: $\hat{P}_{i2}, \hat{P}_{j2}$ – the element's forces collinear to y_2; $\hat{P}_{i6}, \hat{P}_{j6}$ – the element's torques collinear to y_1.

Stepping next to, the method most fundamental assumption, it states that, when a continuous characteristics is extend on the element, its value at a selected point $\boldsymbol{A}$ can be approximated, and a product of some shape functions and the element nodal values can be used for approximation. The introduced shape functions (in general polynomials) are based on the considered point relative position (in respect to the element nodes). As some simplification error is associated with the approximation, the elements size should be low to minimize it. According to it, when the element motion is considered, displacements of a selected point $\boldsymbol{A}$ can be expressed as

$$\hat{\boldsymbol{q}}^A = \hat{\boldsymbol{N}}_e^A \, \hat{\boldsymbol{q}}_{\boldsymbol{e}} \tag{10}$$

where: $\hat{\boldsymbol{N}}_e^A$ – matrix of the considered shape functions.

Afterwards, linear deformations of the element, $\boldsymbol{\varepsilon}^A$, can be obtained when differential relation are used. It leads to [9, 10]

$$\hat{\boldsymbol{\varepsilon}}^A = \hat{\boldsymbol{B}}_e^A \, \hat{\boldsymbol{q}}_{\boldsymbol{e}} \quad : \tag{11a}$$

[1] *All elements of these matrices are geometrical vectors*

$$\boldsymbol{B}_l^A = \begin{bmatrix} \partial/\partial\hat{x}_1 & 0 & 0 & \partial/\partial\hat{x}_2 & 0 & \partial/\partial\hat{x}_3 \\ 0 & \partial/\partial\hat{x}_2 & 0 & \partial/\partial\hat{x}_1 & \partial/\partial\hat{x}_3 & 0 \\ 0 & 0 & \partial/\partial\hat{x}_3 & 0 & \partial/\partial\hat{x}_2 & \partial/\partial\hat{x}_1 \end{bmatrix} \boldsymbol{N}_e^A \tag{11b}$$

Then, when the beam element is considered, cubic functions are used as the shape functions are. The required matrix is [9, 10]

$$\widehat{N}_e(\zeta) = \begin{bmatrix} 2\zeta^3 - 3\zeta^2 + 1 & l_e(\zeta^3 - 2\zeta^2 + \zeta) & -2\zeta^3 + 3\zeta^2 & l_e(\zeta^3 - \zeta^2) \\ \dfrac{6(\zeta^2 - \zeta)}{l} & 3\zeta^2 - 4\zeta + 1 & \dfrac{6(-\zeta^2 + \zeta)}{l} & 3\zeta^2 - 2\zeta \end{bmatrix}, \tag{12}$$

where: $\zeta = \hat{x}_1 / l$ - point's relative position.

According to it, displacements and velocities of the selected point $\boldsymbol{A}$ (Fig. 4) are [9, 10]:

$$col(\hat{q}_{A2}, \hat{q}_{A6}) = \widehat{\boldsymbol{N}}_e(\zeta^A) \cdot \hat{\boldsymbol{q}}_e \;, \quad col(\dot{\hat{q}}_{A2}, \dot{\hat{q}}_{A6}) = \widehat{\boldsymbol{N}}_e(\zeta^A) \cdot \dot{\hat{\boldsymbol{q}}}_e \tag{13}$$

Next, for the planar state of the stresses, the stress/strain relation is [9, 10]

$$\boldsymbol{\sigma}^A = \boldsymbol{D}_e \cdot \boldsymbol{\varepsilon}^A \quad : \quad \boldsymbol{D}_e = \frac{E}{1-\upsilon^2} \begin{bmatrix} 1 & \upsilon & 0 \\ & 1 & 0 \\ sym. & & (1-\upsilon)/2 \end{bmatrix} \tag{14}$$

where: E – modulus of elasticity; υ - Poisson's number,

and the total kinetic energy, as well as potential energy can be written for the element as [9, 10]:

$$E_e = \tfrac{1}{2} \dot{\boldsymbol{q}}_e^T \cdot \boldsymbol{M}_e \cdot \dot{\boldsymbol{q}}_e \; : \; \boldsymbol{M}_e = \tfrac{1}{2} \rho \int_{x_e} \int_{y_e} \int_{z_e} N_e^T \cdot N_e \cdot dx \cdot dy \cdot dz \; ; \tag{15a}$$

$$V_e = \tfrac{1}{2} \boldsymbol{q}_e^T \cdot \boldsymbol{K}_e \cdot \boldsymbol{q}_e \; : \; \boldsymbol{K}_e = \tfrac{1}{2} \int_{x_e} \int_{y_e} \int_{z_e} \boldsymbol{B}_l^T \cdot \boldsymbol{D}_e \cdot \boldsymbol{B}_l \cdot dx \cdot dy \cdot dz \, . \tag{15b}$$

When the beam element is considered, the introduced matrices are [9, 10]:

$$\hat{\boldsymbol{M}}_e = \frac{\rho F l}{420} \begin{bmatrix} 156 & 22l & 54 & -13l \\ & 4l^2 & 13l & -3l^2 \\ & & 156 & -22l \\ sym. & & & 4l^2 \end{bmatrix}, \quad \hat{\boldsymbol{K}}_e = \frac{EJ}{l^3} \begin{bmatrix} 12 & 6l & -12 & 6l \\ & 4l^2 & -6l & 2l^2 \\ & & 12 & -6l \\ sym. & & & 4l^2 \end{bmatrix}. \tag{16}$$

where: ρ – density of the element's material; F – size of the cross section; J – geometrical moment of the cross section.

To add some damping properties, a damping matrix is introduced, and approximated as proportional to the mass and the elasticity matrices [9, 10]

$$\hat{\boldsymbol{B}}_e = \alpha \cdot \hat{\boldsymbol{M}}_e + \beta \cdot \hat{\boldsymbol{K}}_e \; . \tag{17}$$

Equations (8-17) are expressed in elements coordinate systems. They have to be transformed to the global system. As the systems are collinear, identity matrix transformation are used. Next, vectors of nodes displacements and vectors of nodes loads are collected in global matrices [9, 10]:

$$\boldsymbol{q}_c^* = col(\boldsymbol{q}_i) \quad ; \quad \boldsymbol{P}_c^* = col(\boldsymbol{P}_i) \quad : \quad i = 1,2,\ldots,w \,, \tag{18}$$

where: $\boldsymbol{q}_i$- vector of i^{th} node's displacements; $\boldsymbol{P}_i$ - vector of i^{th} node's loads.

For the local mass, damping and stiffness matrices, blocs corresponding to nodes are selected. At their global versions, corresponding cells are placed at the crossing cells of rows and columns with numbers matching to the element nodes. The rest of the elements are kept to be zero.

In the next step, the matrices at the system coordinates are summed over the full set of the system elements. As a result, system global matrices are obtained. Finally rows and columns corresponding to locked nodes are cut out from the global matrices, and final form of dynamics equations is [7, 9]

$$\boldsymbol{M}^c \cdot \ddot{\boldsymbol{q}}^c + \boldsymbol{B}^c \cdot \dot{\boldsymbol{q}}^c + \boldsymbol{K}^c \cdot \boldsymbol{q}^c = \boldsymbol{Q}^c \, . \tag{19}$$

4. Constraint equations

In the papers, a point contact is considered between the multibody system and the finite element model. Permanent slip with friction is considered at the contact point (value of the velocity can vary, but the velocity direction is constant). The shape of the finite element differs from a straight line. Thus an inclination angle α (Fig. 5) describes direction tangent to the profile at the contact point. With the introduced angle, the components of the tangent and the normal vectors obtained in the contact point (express in the global system) can be written:

$$\boldsymbol{t}^* = [1\,,\; tan(\alpha)]^{\mathrm{T}} \quad ; \quad \boldsymbol{n}^* = [-tan(\alpha)\,,\;\; 1]^{\mathrm{T}} \,, \tag{20}$$

and when normalized to unit vectors, ones get

$$\boldsymbol{t} = k\,\boldsymbol{t}^* \quad ; \quad \boldsymbol{n} = k\,\boldsymbol{n} \quad : \qquad k = 1/\sqrt{1 + tan^2\,\alpha} \, . \tag{21}$$

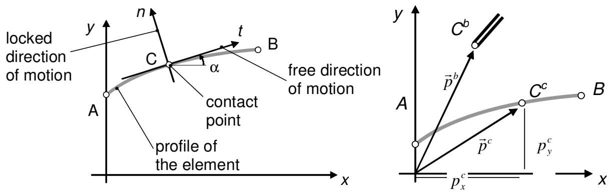

Figure 5: the contact point at the fine element

To obtain the constraint equations, positions of the contact points should be projected on the tangent and the normal directions for the finite element and the multibody points. The edge contact is considered at the multibody structure, thus its local position (at the final body of the multibody structure) is known a priori. Thus, the considered projections are:

$$p_t^b = \vec{t} \circ \vec{p}^b \quad ; \quad p_n^b = \vec{n} \circ \vec{p}^b \quad ; \quad p_t^c = \vec{t} \circ \vec{p}^c \quad ; \quad p_n^c = \vec{n} \circ \vec{p}^c \tag{22a}$$

thus,

$$p_t^b = k\,(p_x^b + p_y^b \cdot tan\,\alpha)\,; \qquad p_n^b = k\,(p_y^b - p_x^b \cdot tan\,\alpha)\,; \tag{22b}$$

$$p_t^c = k\,(p_x^c + p_y^c \cdot tan\,\alpha)\,; \qquad p_n^c = k\,(p_y^c - p_x^c \cdot tan\,\alpha)\,. \tag{22c}$$

As both the points coincide, the constraint equations are:

$$h_1 = p_n^b - p_n^c = k\,(\,(p_y^b - p_y^c) - (p_x^b - p_x^c) \cdot tan\,\alpha) = 0\,; \tag{23a}$$

$$h_2 = p_t^b - p_t^c = k\,(\,(p_x^b - p_x^c) + (p_y^b - p_y^c) \cdot tan\,\alpha) = 0\,; \tag{23b}$$

The obtained set can be express in a matrix form

$$\begin{bmatrix} h_1 \\ h_2 \end{bmatrix} = k \begin{bmatrix} -tan\,\alpha & 1 \\ 1 & tan\,\alpha \end{bmatrix} \cdot \begin{bmatrix} p_x^b - p_x^c \\ p_y^b - p_y^c \end{bmatrix} = \begin{bmatrix} 0 \\ 0 \end{bmatrix}; \tag{24}$$

As the square matrix is not singular, its can be written as

$$\begin{bmatrix} h_x \\ h_y \end{bmatrix} = \begin{bmatrix} p_x^b - p_x^c \\ p_y^b - p_y^c \end{bmatrix} = k^{-1} \begin{bmatrix} -\tan\alpha & 1 \\ 1 & \tan\alpha \end{bmatrix}^{-1} \cdot \begin{bmatrix} 0 \\ 0 \end{bmatrix} = \begin{bmatrix} 0 \\ 0 \end{bmatrix}; \tag{25}$$

Equation (25) allows us to solve the constraint equations, at level of coordinates of the reference system, i.e. when kinematics is considered, only. The obtained form of (25) is equivalent to the initial form (23). Some kinematical relations from (25) are useful. For example, according to (11) and the definition of the ζ variable, as presented at (12), the constraints (25) can be written as:

$$h_x = (p_x^b - p_x^c) = p_x^b - \zeta \cdot l = 0; \tag{26a}$$

$$h_y = (p_y^b - p_y^c) = p_y^b - \boldsymbol{N}^y \cdot \boldsymbol{q}^c = 0, \tag{26b}$$

where: $\boldsymbol{N}^y$ – matrix build of the shape functions used to describe element's vertical deformations.

Now, Eq. (26a) can be used to determinate the auxiliary variable ζ (it locates the contact point at the finite element). The considered parameter is a geometrical parameter (i.e. not a material point at the finite element), thus, when time derivatives of (26a) are calculated as:

$$\dot{h}_x = (\dot{p}_x^b - \dot{p}_x^c) = \dot{p}_x^b - \dot{\zeta} \cdot l = \boldsymbol{J}_x^b \cdot \dot{\boldsymbol{q}}_b - \dot{\zeta} \cdot l = 0; \tag{27a}$$

$$\ddot{h}_x = (\ddot{p}_x^b - \ddot{p}_x^c) = \ddot{p}_x^b - \ddot{\zeta} \cdot l = \boldsymbol{J}_x^b \cdot \ddot{\boldsymbol{q}}_b + A_x^b - \ddot{\zeta} \cdot l = 0, \tag{27b}$$

they do not indicate that the slip at the contact point is absent. They represent geometrical changes at position of the contact point. Basically, time derivatives of ζ can be obtain from (27).

It has to be underlined that Eq. (26) can be restricted to kinematical considerations only. In the dynamic analysis, some details (Lagrange multipliers interpretations) differ. Thus the initial form (23) will be considered in the next operations. First, the first time derivative of (23a) is

$$\begin{aligned} \dot{h}_1 &= \dot{k}\,((p_y^b - p_y^c) - (p_x^b - p_x^c) \cdot \tan\alpha) + \\ &+ k\,((\dot{p}_y^b - \dot{p}_y^c) - (\dot{p}_x^b - \dot{p}_x^c) \cdot \tan\alpha) - k\,((p_x^b - p_x^c) \cdot \dot{\tan}\,\alpha) = 0, \end{aligned} \tag{28}$$

However, when the constraint equations are satisfied at position level, i.e. when the Eqs. (23a) and (25) are satisfied, the parenthesis at the first and third summand equal zero, thus

$$\dot{h}_1 = k\,((\dot{p}_y^b - \dot{p}_y^c) - (\dot{p}_x^b - \dot{p}_x^c) \cdot \tan\alpha) = 0; \tag{29}$$

The time derivative at (29) can be calculated from the multibody and from the finite element kinematics (i.e. from the time derivative of (11a)). Then, Eq. (29) can be written as

$$\dot{h}_1 = k((\boldsymbol{J}_y^b \cdot \dot{\boldsymbol{q}}^b - \boldsymbol{N}^y \cdot \dot{\boldsymbol{q}}^c - \boldsymbol{N}_{(\zeta)}^y \cdot \dot{\zeta} \cdot \boldsymbol{q}^c) - (\dot{p}_x^b - \dot{\zeta} \cdot l) \cdot \tan\alpha) = 0; \tag{30}$$

where

$$\boldsymbol{N}_{(\zeta)}^y = \frac{\partial \boldsymbol{N}^y}{\partial \zeta} = \begin{bmatrix} 6\zeta^2 - 6\zeta & l(3\zeta^2 - 4\zeta + 1) & -6\zeta^2 + 6\zeta & l(3\zeta^2 - 2\zeta) \\ \frac{6(2\zeta - 1)}{l} & 6\zeta - 4 & \frac{6(-2\zeta + 1)}{l} & 6\zeta - 2 \end{bmatrix}; \tag{31}$$

Next according to (27a), Eq. (30) can be modified to:

$$\dot{h}_1 = k\,(\boldsymbol{J}_y^b \cdot \dot{\boldsymbol{q}}^b - \boldsymbol{N}^y \cdot \dot{\boldsymbol{q}}^c - \boldsymbol{N}_{(\zeta)}^y \cdot \dot{\zeta} \cdot \boldsymbol{q}^c) = 0; \tag{32}$$

$$\dot{h}_1 = k\,(\boldsymbol{J}_y^b - \tfrac{1}{l} \cdot \boldsymbol{N}_{(\zeta)}^y \cdot \boldsymbol{q}^c \cdot \boldsymbol{J}_x^b) \cdot \dot{\boldsymbol{q}}^b - k\,\boldsymbol{N}^y \cdot \dot{\boldsymbol{q}}^c = 0; \tag{33}$$

$$\dot{h}_1 = \boldsymbol{J}_n^b \cdot \dot{\boldsymbol{q}}^b + \boldsymbol{J}_n^c \cdot \dot{\boldsymbol{q}}^c = 0: \; \boldsymbol{J}_n^b = k(\boldsymbol{J}_y^b - \tfrac{1}{l} \cdot \boldsymbol{N}_{(\zeta)}^y \cdot \boldsymbol{q}^c \cdot \boldsymbol{J}_x^b); \; \boldsymbol{J}_n^c = -k \cdot \boldsymbol{N}^y \tag{34}$$

The obtained equation (34) can be used to eliminate one of the velocities of the system variables. To eliminate accelerations, second time derivative is necessary. It can be calculated as

$$\begin{aligned} \ddot{h}_1 &= \ddot{k}\,((p_y^b - p_y^c) - (p_x^b - p_x^c) \cdot \tan\alpha) + \\ &+ 2\dot{k}\,((\dot{p}_y^b - \dot{p}_y^c) - (\dot{p}_x^b - \dot{p}_x^c) \cdot \tan\alpha - (p_x^b - p_x^c) \cdot \dot{\tan}\,\alpha) + \\ &+ k\,((\ddot{p}_y^b - \ddot{p}_y^c) - (\ddot{p}_x^b - \ddot{p}_x^c) \cdot \tan\alpha - (p_x^b - p_x^c) \cdot \ddot{\tan}\,\alpha + \\ &- 2(\dot{p}_x^b - \dot{p}_x^c) \cdot \dot{\tan}\,\alpha) = 0. \end{aligned} \tag{35}$$

However, as the constraint equations are satisfied at the position and velocity level, i.e. when the constraint equations (23a), (25), (27) and (29) are satisfied, the derivative is reduced to

$$\ddot{h}_1 = k\,((\ddot{p}_y^b - \ddot{p}_y^c) - (\ddot{p}_x^b - \ddot{p}_x^c) \cdot \tan\alpha) = 0. \tag{36}$$

Next, as Eq. (27b) is satisfied, it leads to

$$\ddot{h}_1 = k\,(\ddot{p}_y^b - \ddot{p}_y^c) = 0. \tag{37}$$

Applying the multibody kinematics as well as the finite element kinematics, Eq. (36) can be written as

$$\ddot{h}_1 = k\,(\boldsymbol{J}_y^b \cdot \ddot{\boldsymbol{q}}^b + A_y^b - \boldsymbol{N}^y \cdot \ddot{\boldsymbol{q}}^c - 2\dot{\boldsymbol{N}}^y \cdot \dot{\boldsymbol{q}}^c - \ddot{\boldsymbol{N}}^y \cdot \boldsymbol{q}^c) = 0. \tag{38}$$

$$\begin{aligned} \ddot{h}_1 = k\,(&\boldsymbol{J}_y^b \cdot \ddot{\boldsymbol{q}}^b + A_y^b - \boldsymbol{N}^y \cdot \ddot{\boldsymbol{q}}^c - 2\boldsymbol{N}_{(\zeta)}^y \cdot \dot{\zeta} \cdot \dot{\boldsymbol{q}}^c + \\ &- \tfrac{d}{dt}(\boldsymbol{N}_{(\zeta)}^y \cdot \dot{\zeta}) \cdot \boldsymbol{q}^c) = 0. \end{aligned} \tag{39}$$

$$\begin{aligned} \ddot{h}_1 = k\,(&\boldsymbol{J}_y^b \cdot \ddot{\boldsymbol{q}}^b + A_y^b - \boldsymbol{N}^y \cdot \ddot{\boldsymbol{q}}^c - 2\boldsymbol{N}_{(\zeta)}^y \cdot \dot{\zeta} \cdot \dot{\boldsymbol{q}}^c + \\ &- (\boldsymbol{N}_{(\zeta\zeta)}^y \cdot \dot{\zeta}^2 + \boldsymbol{N}_{(\zeta)}^y \cdot \ddot{\zeta}) \cdot \boldsymbol{q}^c) = 0, \end{aligned} \tag{40}$$

where

$$\boldsymbol{N}_{(\zeta\zeta)}^y = \frac{\partial^2 \boldsymbol{N}^y}{\partial \zeta^2} = \begin{bmatrix} 12\zeta - 6 & l(6\zeta - 4) & -12\zeta + 6 & l(6\zeta - 2) \\ \frac{12}{l} & 6 & \frac{-12}{l} & 6 \end{bmatrix}. \tag{41}$$

Next, when Eq. (27) is used ones can write:

$$\begin{aligned} \ddot{h}_1 = k\,(&\boldsymbol{J}_y^b \cdot \ddot{\boldsymbol{q}}^b + A_y^b - \boldsymbol{N}^y \cdot \ddot{\boldsymbol{q}}^c - \tfrac{2}{l} \cdot \boldsymbol{N}_{(\zeta)}^y \cdot \dot{\boldsymbol{q}}^c \cdot \boldsymbol{J}_x^b \cdot \dot{\boldsymbol{q}}^b + \\ &- (\tfrac{1}{l^2} \cdot \boldsymbol{N}_{(\zeta\zeta)}^y \cdot (\boldsymbol{J}_x^b \cdot \dot{\boldsymbol{q}}^b)^2 + \tfrac{1}{l} \cdot \boldsymbol{N}_{(\zeta)}^y \cdot \boldsymbol{J}_x^b \cdot \ddot{\boldsymbol{q}}^b + \tfrac{1}{l} \cdot \boldsymbol{N}_{(\zeta)}^y \cdot A_x^b) \cdot \boldsymbol{q}^c) = 0; \end{aligned} \tag{42}$$

$$\begin{aligned} \ddot{h}_1 &= k\,((\boldsymbol{J}_y^b + \tfrac{1}{l} \cdot \boldsymbol{N}_{(\zeta)}^y \cdot \boldsymbol{q}^c \cdot \boldsymbol{J}_x^b) \cdot \ddot{\boldsymbol{q}}^b - \boldsymbol{N}^y \cdot \ddot{\boldsymbol{q}}^c \\ &+ A_y^b - (\tfrac{1}{l} \cdot A_x^b \cdot \boldsymbol{N}_{(\zeta)}^y - \tfrac{2}{l}(\boldsymbol{J}_x^b \dot{\boldsymbol{q}}^b) \cdot \boldsymbol{N}_{(\zeta)}^y - \tfrac{1}{l^2}(\boldsymbol{J}_x^b \cdot \dot{\boldsymbol{q}}^b)^2 \cdot \boldsymbol{N}_{(\zeta\zeta)}^y) \cdot \boldsymbol{q}^c) = 0, \end{aligned} \tag{43}$$

and, with the symbols introduced in (34), ones obtain

$$\ddot{h}_1 = \boldsymbol{J}_n^b \cdot \ddot{\boldsymbol{q}}^b + \boldsymbol{J}_n^c \cdot \ddot{\boldsymbol{q}}^c + A_n = 0, \tag{44}$$

where

$$A_n = A_y^b - (\tfrac{1}{l} \cdot A_x^b \cdot \boldsymbol{N}_{(\zeta)}^y - \tfrac{2}{l}(\boldsymbol{J}_x^b \dot{\boldsymbol{q}}^b) \cdot \boldsymbol{N}_{(\zeta)}^y - \tfrac{1}{l^2}(\boldsymbol{J}_x^b \cdot \dot{\boldsymbol{q}}^b)^2 \cdot \boldsymbol{N}_{(\zeta\zeta)}^y) \cdot \boldsymbol{q}^c). \tag{45}$$

At the end, let us to underline the normal direction formulation (32) and (37) differ from the reference system formulation by a presence of the scale coefficient k, only. As different from zero, it can be omitted in the kinematical considerations. However, in the dynamical considerations, the coefficient has to be considered in the Jacobian definition.

5. Slip and its direction

The introduced constraint equations related velocities of geometrical points. By contrast, in the next equations, velocities of the material points are taken into account. Before the future investigations, let us to note, that the *x* component of the material point velocity equals zero for the finite element points (the elements deform in the vertical direction only). Thus, the normal components of the point velocities can be expressed as:

$$v_n^b = \vec{n} \circ \vec{v}^b = k \begin{bmatrix} -tan\,\alpha & 1 \end{bmatrix} \cdot \begin{bmatrix} v_x^b \\ v_y^b \end{bmatrix} = k\,(\boldsymbol{J}_y^b \cdot \dot{\boldsymbol{q}}^b - \boldsymbol{J}_x^b \cdot \dot{\boldsymbol{q}}^b \cdot tan(\alpha))\,; \quad (46)$$

$$v_n^c = \vec{n} \circ \vec{v}^c = k \begin{bmatrix} -tan\,\alpha & 1 \end{bmatrix} \cdot \begin{bmatrix} 0 \\ v_x^c \end{bmatrix} = k\, v_y^c = k\, \boldsymbol{N}^y \cdot \dot{\boldsymbol{q}}^c\,, \quad (47)$$

and the normal component of the relative velocity is

$$\Delta v_n = v_n^b - v_n^c = k\,(\boldsymbol{J}_y^b \cdot \dot{\boldsymbol{q}}^b - \boldsymbol{J}_x^b \cdot \dot{\boldsymbol{q}}^b \cdot tan(\alpha) - \boldsymbol{N}^y \cdot \dot{\boldsymbol{q}}^c)\,; \quad (48)$$

With the tangent of inclination defined by the second row of (12) (when comprised with the first row of (31)), ones can write

$$\Delta v_n = k\,(\,\boldsymbol{J}_y^b - \tfrac{1}{l} \cdot \boldsymbol{N}_{(\zeta)}^y \cdot \boldsymbol{q}^c \cdot \boldsymbol{J}_x^b\,) \cdot \dot{\boldsymbol{q}}^b - k\, \boldsymbol{N}^y \cdot \dot{\boldsymbol{q}}^c\,. \quad (49)$$

According to Eq. (33), the component equals zero. However, a detail has to be underlined. Equation (33) was deliberated for the geometrical points, Eq. (49) states zero relative velocity for the material points, too.

By analogy, tangent slip can be determined. The tangent components of the velocities can be expressed as:

$$v_t^b = \vec{t} \circ \vec{v}^b = k \begin{bmatrix} 1 & tan\,\alpha \end{bmatrix} \cdot \begin{bmatrix} v_x^b \\ v_y^b \end{bmatrix} = k\,(\boldsymbol{J}_x^b \cdot \dot{\boldsymbol{q}}^b + \boldsymbol{J}_y^b \cdot \dot{\boldsymbol{q}}^b \cdot tan(\alpha))\,; \quad (50)$$

$$v_t^c = \vec{t} \circ \vec{v}^c = k \begin{bmatrix} 1 & tan\,\alpha \end{bmatrix} \cdot \begin{bmatrix} 0 \\ v_y^c \end{bmatrix} = k\,(\boldsymbol{N}^y \cdot \dot{\boldsymbol{q}}^c \cdot tan(\alpha))\,, \quad (51)$$

thus, the tangent component of the relative velocity is

$$\Delta v_t = v_t^b - v_t^c = k\,(\boldsymbol{J}_x^b \cdot \dot{\boldsymbol{q}}^b + \boldsymbol{J}_y^b \cdot \dot{\boldsymbol{q}}^b \cdot tan(\alpha) - \boldsymbol{N}^y \cdot \dot{\boldsymbol{q}}^c \cdot tan(\alpha))\,. \quad (52)$$

Next, with the tangent of inclination defined by the second row of (12) (compared with the first row of (31)), ones can write

$$\Delta v_t = v_t^b - v_t^c = k\,(\boldsymbol{J}_x^b \cdot \dot{\boldsymbol{q}}^b + \boldsymbol{J}_y^b \cdot \dot{\boldsymbol{q}}^b \cdot \boldsymbol{N}_{(\zeta)}^y \cdot \boldsymbol{q}^c - \boldsymbol{N}^y \cdot \dot{\boldsymbol{q}}^c \cdot \boldsymbol{N}_{(\zeta)}^y \cdot \boldsymbol{q}^c)\,. \quad (53)$$

More useful form can be obtained when same zero operations are added

$$\Delta v_t = k\,(\boldsymbol{J}_x^b \cdot \dot{\boldsymbol{q}}^b + \boldsymbol{N}_{(\zeta)}^y \cdot \dot{\zeta} \cdot \boldsymbol{q}^c) + k\,(\boldsymbol{J}_y^b \cdot \dot{\boldsymbol{q}}^b \cdot tan(\alpha) - \boldsymbol{N}^y \cdot \dot{\boldsymbol{q}}^c \cdot tan(\alpha) - \boldsymbol{N}_{(\zeta)}^y \cdot \dot{\zeta} \cdot \boldsymbol{q}^c)\,, \quad (54)$$

then, when the constraint equations are satisfied at velocity level, according to Eq. (32), it can be written as

$$\Delta v_t = k\,(\boldsymbol{J}_x^b \cdot \dot{\boldsymbol{q}}^b + \boldsymbol{N}_{(\zeta)}^y \cdot \dot{\zeta} \cdot \boldsymbol{q}^c) \quad (55)$$

and according to (27a), ones can rewrite it as

$$\Delta v_t = k\,(\boldsymbol{J}_x^b \cdot \dot{\boldsymbol{q}}^b + \tfrac{1}{l} \boldsymbol{N}_{(\zeta)}^y \cdot \boldsymbol{q}^c \cdot (\boldsymbol{J}_x^b \cdot \dot{\boldsymbol{q}}^b)) \quad (56)$$

$$\Delta v_t = \boldsymbol{J}_t^{\Delta} \cdot \dot{\boldsymbol{q}}^b \quad : \quad \boldsymbol{J}_t^{\Delta} = k\,(\boldsymbol{J}_x^b + \tfrac{1}{l} \boldsymbol{N}_{(\zeta)}^y \cdot \boldsymbol{q}^c \cdot \boldsymbol{J}_x^b) \quad (57)$$

In general, the obtained tangent component differs from zero. However, only its sign will be considered in the future calculations (to determine direction of the friction force).

6. Ideal (friction free) contact

To get some general overview, a simpler (friction free) contact is presented initially. According to (7) and (19) dynamics can be establish for the multibody and the continuous systems. Next the constraint equation (23) and the constraint interactions have to be introduced. According to the Lagrange multipliers technique, the dynamics equations convert to differentially-algebraic form:

$$\boldsymbol{M}^b \cdot \ddot{\boldsymbol{q}}^b + \boldsymbol{F}^b = \boldsymbol{Q}^b + \boldsymbol{J}_n^{bT} \cdot \lambda\,; \quad (58)$$

$$\boldsymbol{M}^c \cdot \ddot{\boldsymbol{q}}^c + \boldsymbol{D}^c \cdot \dot{\boldsymbol{q}}^c + \boldsymbol{K}^c \cdot \boldsymbol{q}^c = \boldsymbol{Q}^c + \boldsymbol{J}_n^{cT} \cdot \lambda\,; \quad (59)$$

$$h_y = p_y^b - \boldsymbol{N}^y \cdot \boldsymbol{q}^c = 0\,; \quad (60)$$

$$\dot{h}_1 = \boldsymbol{J}_n^b \cdot \dot{\boldsymbol{q}}^b + \boldsymbol{J}_n^c \cdot \dot{\boldsymbol{q}}^c = 0\,; \quad (61)$$

$$\ddot{h}_1 = \boldsymbol{J}_n^b \cdot \ddot{\boldsymbol{q}}^b + \boldsymbol{J}_n^c \cdot \ddot{\boldsymbol{q}}^c + A_n = 0\,. \quad (62)$$

The introduce Lagrange multipliers express the constraint interactions. According to the used constraints formulas, the multipliers refer directly to the contact point normal force.

7. Generalized forces associated to the friction force

The friction force is estimated according to the classical Coulomb friction hypothesis. It leads to

$$\vec{f}_T = -sign(\,\Delta v_t^b\,) \cdot \mu \cdot \lambda \cdot \vec{t} \quad (63)$$

The introduced friction force affects both of the systems (i.e. the multibody and the continuous system). For the multibody system, virtual powers associated to the friction force equals:

$$\begin{aligned} P_T^b &= \vec{f}_t \circ \vec{v}^b = -sign(\Delta v_t^b) \cdot \mu \cdot \lambda \cdot \vec{t} \circ \vec{v}^b = \\ &= -sign(\Delta v_t^b) \cdot \mu \cdot \lambda \cdot k \cdot (v_x^b + v_y^b \cdot tan\,\alpha\,) = \\ &= -sign(\Delta v_t^b) \cdot \mu \cdot \lambda \cdot k \cdot (\boldsymbol{J}_x^b + \boldsymbol{J}_y^b \cdot tan\,\alpha\,) \cdot \dot{\boldsymbol{q}}^b = \boldsymbol{Q}_T^{bT} \cdot \dot{\boldsymbol{q}}^b \end{aligned} \quad (64)$$

Simultaneously, for the continuous system the power is

$$\begin{aligned} P_T^c &= \vec{f}_T \circ \vec{v}^c = -sign(\Delta v_t^c) \cdot \mu \cdot \lambda \cdot \vec{t} \circ \vec{v}^c = \\ &= sign(\Delta v_t^b) \cdot \mu \cdot \lambda \cdot k \cdot (v_y^c \cdot tan\,\alpha\,) = \\ &= sign(\Delta v_t^b) \cdot \mu \cdot \lambda \cdot k \cdot (\boldsymbol{N}_y \cdot tan\,\alpha\,) \cdot \dot{\boldsymbol{q}}^c = \boldsymbol{Q}_T^{cT} \cdot \dot{\boldsymbol{q}}^c \end{aligned} \quad (65)$$

where: $\vec{v}^c$ - velocity of the beam contact point; $\vec{v}^b$ - velocity of the multibody contact point;

Within the introduced velocity equations, depending on the used reference system, two opposite relative velocities are used. Their definitions are

$$\Delta v_t^b = v_t^b - v_t^c \quad ; \quad \Delta v_t^c = -\Delta v_t^b = v_t^c - v_t^b \quad (66)$$

Then, according to Eqs. (64) and (65), the announced generalize forces can be express as:

$$\boldsymbol{Q}_T^b = -sign(\Delta v_t^b)\cdot \mu \cdot k \cdot (\boldsymbol{J}_x^{bT} + \boldsymbol{J}_y^{bT}\cdot tan\,\alpha)\cdot \lambda = \boldsymbol{J}_T^{bT}\cdot \lambda\,; \tag{67a}$$

$$\boldsymbol{Q}_T^c = sign(\Delta v_t^b)\cdot \mu \cdot k \cdot (\boldsymbol{N}_y^T\cdot tan\,\alpha)\cdot \lambda = \boldsymbol{J}_T^{cT}\cdot \lambda\,. \tag{67b}$$

where:

$$\boldsymbol{J}_T^b = -sign(\Delta v_t^b)\cdot \mu \cdot k \cdot (\boldsymbol{J}_x^b + \boldsymbol{J}_y^b\cdot tan\,\alpha)\,; \tag{68a}$$

$$\boldsymbol{J}_T^c = sign(\Delta v_t^b)\cdot \mu \cdot k \cdot (\boldsymbol{N}_y\cdot tan\,\alpha)\,. \tag{68b}$$

Let us remain, the multibody system power dose not equal to the continuous system one, as part of it is dissipated on the slip velocity. Despite it, action of the friction force is not limited to the energy dissipation. The energy transfer between the systems is performed, too.

8. Dynamics equations

As the additional friction force (explicitly dependent on the Lagrange multipliers) is present in the system, their generalized forces have to be introduced and, Eqs. (58) and (59) become

$$\boldsymbol{M}^b\cdot\ddot{\boldsymbol{q}}^b + \boldsymbol{F}^b = \boldsymbol{Q}^b + \boldsymbol{J}_n^{bT}\cdot\lambda + \boldsymbol{Q}_T^b\,; \tag{69a}$$

$$\boldsymbol{M}^c\cdot\ddot{\boldsymbol{q}}^c + \boldsymbol{D}^c\cdot\dot{\boldsymbol{q}}^c + \boldsymbol{K}^c\cdot\boldsymbol{q}^c = \boldsymbol{Q}^c + \boldsymbol{J}_n^{cT}\cdot\lambda + \boldsymbol{Q}_T^c\,; \tag{69b}$$

However, when Eq. (67) is used, Eq. (69) can be written as

$$\boldsymbol{M}^b\cdot\ddot{\boldsymbol{q}}^b + \boldsymbol{F}^b = \boldsymbol{Q}^b + \boldsymbol{J}_n^{bT}\cdot\lambda + \boldsymbol{J}_T^{bT}\cdot\lambda\,; \tag{70a}$$

$$\boldsymbol{M}^c\cdot\ddot{\boldsymbol{q}}^c + \boldsymbol{D}^c\cdot\dot{\boldsymbol{q}}^c + \boldsymbol{K}^c\cdot\boldsymbol{q}^c = \boldsymbol{Q}^c + \boldsymbol{J}_n^{cT}\cdot\lambda + \boldsymbol{J}_T^{bT}\cdot\lambda\,, \tag{70b}$$

and then, they can be converted to the form

$$\boldsymbol{M}^b\cdot\ddot{\boldsymbol{q}}^b + \boldsymbol{F}^b = \boldsymbol{Q}^b + \boldsymbol{J}_\Sigma^{bT}\cdot\lambda\,; \tag{71a}$$

$$\boldsymbol{M}^c\cdot\ddot{\boldsymbol{q}}^c + \boldsymbol{D}^c\cdot\dot{\boldsymbol{q}}^c + \boldsymbol{K}^c\cdot\boldsymbol{q}^c = \boldsymbol{Q}^c + \boldsymbol{J}_\Sigma^{cT}\cdot\lambda\,, \tag{71b}$$

where:

$$\boldsymbol{J}_\Sigma^b = \boldsymbol{J}_n^b + \boldsymbol{J}_T^b \quad ; \qquad \boldsymbol{J}_\Sigma^c = \boldsymbol{J}_n^c + \boldsymbol{J}_T^c\,; \tag{71c}$$

The introduced dynamics equations have to be joined with the constraint equations (60)-(62). As previously, it leads to a set of differential-algebraic equations. To obtain the differential form of the dynamics equations, a modified partitioning method is necessary. The coefficients matrix in front of the multipliers is no more the Jacobian matrix of the constraint equations. Moreover, in the presently considered case, the depended coordinates are associated to the multibody system, only. Additional numerical benefits can be obtained, as the dynamics equations of the multibody system are independent on the coordinates of the deformable beam (and vice-verso). According to it, Eq. (62) can be written

$$\boldsymbol{J}_v^b\cdot\ddot{\boldsymbol{q}}_v^b + \boldsymbol{J}_u^b\cdot\ddot{\boldsymbol{q}}_u^b + \boldsymbol{J}_n^c\cdot\ddot{\boldsymbol{q}}^c + A_n = 0 \quad : \quad \boldsymbol{J}_n^b = [\boldsymbol{J}_u^b\ ,\ \boldsymbol{J}_v^b]\,; \tag{72}$$

where: $\boldsymbol{q}_u^b$ - dependent coordinates; $\boldsymbol{q}_v^b$ - independent coordinates.

Solving it in respect to dependent coordinates, it states to

$$\ddot{\boldsymbol{q}}_u^b = -\boldsymbol{B}_1\cdot\ddot{\boldsymbol{q}}_v^b - \boldsymbol{B}_2\cdot\ddot{\boldsymbol{q}}^c - \boldsymbol{B}_3\,, \tag{73a}$$

where:

$$\boldsymbol{B}_1 = (\boldsymbol{J}_u^b)^{-1}\cdot\boldsymbol{J}_v^b \quad ; \quad \boldsymbol{B}_2 = (\boldsymbol{J}_u^b)^{-1}\cdot\boldsymbol{J}_n^c \quad ; \quad \boldsymbol{B}_3 = (\boldsymbol{J}_u^b)^{-1}\cdot A_n \tag{73b}$$

Imposing the same partitioning to the rows of the dynamics equations, the dynamics equation (71a) can be partitioned on:

$$\boldsymbol{M}_{uu}^b\cdot\ddot{\boldsymbol{q}}_u^b + \boldsymbol{M}_{uv}^b\cdot\ddot{\boldsymbol{q}}_v^b + \boldsymbol{F}_u^b = \boldsymbol{Q}_u^b + \boldsymbol{J}_{u\Sigma}^{bT}\cdot\lambda\,; \tag{74a}$$

$$\boldsymbol{M}_{vu}^b\cdot\ddot{\boldsymbol{q}}_u^b + \boldsymbol{M}_{vv}^b\cdot\ddot{\boldsymbol{q}}_v^b + \boldsymbol{F}_v^b = \boldsymbol{Q}_v^b + \boldsymbol{J}_{v\Sigma}^{bT}\cdot\lambda\,. \tag{74b}$$

Next, when Eq. (73) is introduced, Eq. (74) is converted to

$$(\boldsymbol{M}_{uv}^b - \boldsymbol{M}_{uu}^b\cdot\boldsymbol{B}_1)\ddot{\boldsymbol{q}}_v^b - \boldsymbol{M}_{uu}^b\cdot\boldsymbol{B}_2\cdot\ddot{\boldsymbol{q}}^c + (\boldsymbol{F}_u^b - \boldsymbol{M}_{uu}^b\cdot\boldsymbol{B}_3) = \boldsymbol{Q}_u^b + \boldsymbol{J}_{u\Sigma}^{bT}\cdot\lambda\,; \tag{75a}$$

$$(\boldsymbol{M}_{vv}^b - \boldsymbol{M}_{vu}^b\cdot\boldsymbol{B}_1)\ddot{\boldsymbol{q}}_v^b - \boldsymbol{M}_{vu}^b\cdot\boldsymbol{B}_2\cdot\ddot{\boldsymbol{q}}^c + (\boldsymbol{F}_v^b - \boldsymbol{M}_{vu}^b\cdot\boldsymbol{B}_3) = \boldsymbol{Q}_v^b + \boldsymbol{J}_{v\Sigma}^{bT}\cdot\lambda \tag{75b}$$

and the Lagrange multiplier is estimated from (75a)

$$\begin{aligned}\lambda = {} & (\boldsymbol{J}_{u\Sigma}^{bT})^{-1}\cdot(\boldsymbol{M}_{uv}^b - \boldsymbol{M}_{uu}^b\cdot\boldsymbol{B}_1)\cdot\ddot{\boldsymbol{q}}_v^b - (\boldsymbol{J}_{u\Sigma}^{bT})^{-1}\cdot\boldsymbol{M}_{uu}^b\cdot\boldsymbol{B}_2\cdot\ddot{\boldsymbol{q}}^c + \\ & + (\boldsymbol{J}_{u\Sigma}^{bT})^{-1}\cdot\boldsymbol{F}_u^b - (\boldsymbol{J}_{u\Sigma}^{bT})^{-1}\cdot\boldsymbol{M}_{uu}^b\cdot\boldsymbol{B}_3 - (\boldsymbol{J}_{u\Sigma}^{bT})^{-1}\cdot\boldsymbol{Q}_u^b\,.\end{aligned} \tag{76}$$

The obtained multipliers can be introduced to (75b) and to (71b). It leads to

$$\begin{aligned}&(\boldsymbol{M}_{vv}^b - \boldsymbol{M}_{vu}^b\cdot\boldsymbol{B}_1)\ddot{\boldsymbol{q}}_v^b - \boldsymbol{M}_{vu}^b\cdot\boldsymbol{B}_2\cdot\ddot{\boldsymbol{q}}^c + (\boldsymbol{F}_v^b - \boldsymbol{M}_{vu}^b\cdot\boldsymbol{B}_3) = \boldsymbol{Q}_v^b + \\ &+ \boldsymbol{J}_{v\Sigma}^{bT}\cdot(\boldsymbol{J}_{u\Sigma}^{bT})^{-1}\cdot(\boldsymbol{M}_{uv}^b - \boldsymbol{M}_{uu}^b\cdot\boldsymbol{B}_1)\ddot{\boldsymbol{q}}_v^b - \boldsymbol{J}_{v\Sigma}^{bT}\cdot(\boldsymbol{J}_{u\Sigma}^{bT})^{-1}\cdot\boldsymbol{M}_{uu}^b\cdot\boldsymbol{B}_2\cdot\ddot{\boldsymbol{q}}^c + \\ &+ \boldsymbol{J}_{v\Sigma}^{bT}\cdot(\boldsymbol{J}_{u\Sigma}^{bT})^{-1}\cdot\boldsymbol{F}_u^b - \boldsymbol{J}_{v\Sigma}^{bT}\cdot(\boldsymbol{J}_{u\Sigma}^{bT})^{-1}\cdot\boldsymbol{M}_{uu}^b\cdot\boldsymbol{B}_3 - \boldsymbol{J}_{v\Sigma}^{bT}\cdot(\boldsymbol{J}_{u\Sigma}^{bT})^{-1}\cdot\boldsymbol{Q}_u^b\,.\end{aligned} \tag{77a}$$

$$\begin{aligned}&\boldsymbol{M}^c\cdot\ddot{\boldsymbol{q}}^c + \boldsymbol{D}^c\cdot\dot{\boldsymbol{q}}^c + \boldsymbol{K}^c\cdot\boldsymbol{q}^c = \boldsymbol{Q}^c + \\ &+ \boldsymbol{J}_n^{cT}\cdot(\boldsymbol{J}_{u\Sigma}^{bT})^{-1}(\boldsymbol{M}_{uv}^b - \boldsymbol{M}_{uu}^b\cdot\boldsymbol{B}_1)\ddot{\boldsymbol{q}}_v^b - \boldsymbol{J}_n^{cT}\cdot(\boldsymbol{J}_{u\Sigma}^{bT})^{-1}\cdot\boldsymbol{M}_{uu}^b\cdot\boldsymbol{B}_2\cdot\ddot{\boldsymbol{q}}^c + \\ &+ \boldsymbol{J}_n^{cT}\cdot(\boldsymbol{J}_{u\Sigma}^{bT})^{-1}\cdot\boldsymbol{F}_u^b - \boldsymbol{J}_n^{cT}\cdot(\boldsymbol{J}_{u\Sigma}^{bT})^{-1}\cdot\boldsymbol{M}_{uu}^b\cdot\boldsymbol{B}_3 - \boldsymbol{J}_n^{cT}\cdot(\boldsymbol{J}_{u\Sigma}^{bT})^{-1}\cdot\boldsymbol{Q}_u^b\,;\end{aligned} \tag{77b}$$

Finally, when coefficient in front of the accelerations are cumulated, ones can write

$$\begin{aligned}&(\boldsymbol{M}_{vv}^b - \boldsymbol{M}_{vu}^b\cdot\boldsymbol{B}_1 - \boldsymbol{B}_4^T\cdot\boldsymbol{M}_{uv}^b + \boldsymbol{B}_4^T\cdot\boldsymbol{M}_{uu}^b\cdot\boldsymbol{B}_1)\ddot{\boldsymbol{q}}_v^b + (\boldsymbol{B}_4^T\cdot\boldsymbol{M}_{uu}^b\cdot\boldsymbol{B}_2 - \boldsymbol{M}_{vu}^b\cdot\boldsymbol{B}_2)\ddot{\boldsymbol{q}}^c \\ &+ (\boldsymbol{F}_v^b - \boldsymbol{B}_4^T\cdot\boldsymbol{F}_u^b - \boldsymbol{M}_{vu}^b\cdot\boldsymbol{B}_3 + \boldsymbol{B}_4^T\cdot\boldsymbol{M}_{uu}^b\cdot\boldsymbol{B}_3) = \boldsymbol{Q}_v^b - \boldsymbol{B}_4^T\cdot\boldsymbol{Q}_u^b\end{aligned} \tag{78a}$$

$$\begin{aligned}&(-\boldsymbol{B}_5\cdot\boldsymbol{M}_{uv}^b + \boldsymbol{B}_5\cdot\boldsymbol{M}_{uu}^b\cdot\boldsymbol{B}_1)\ddot{\boldsymbol{q}}_v^b - \boldsymbol{B}_5\cdot\boldsymbol{F}_u^b + \boldsymbol{B}_5\cdot\boldsymbol{M}_{uu}^b\cdot\boldsymbol{B}_3 \\ &+ (\boldsymbol{M}^c + \boldsymbol{B}_5\cdot\boldsymbol{M}_{uu}^b\cdot\boldsymbol{B}_2)\ddot{\boldsymbol{q}}^c + \boldsymbol{D}^c\cdot\dot{\boldsymbol{q}}^c + \boldsymbol{K}^c\cdot\boldsymbol{q}^c = \boldsymbol{Q}^c - \boldsymbol{B}_5\cdot\boldsymbol{Q}_u^b\,;\end{aligned} \tag{78b}$$

where:

$$\boldsymbol{B}_4 = (\boldsymbol{J}_{u\Sigma}^b)^{-1}\cdot\boldsymbol{J}_{v\Sigma}^b \quad ; \quad \boldsymbol{B}_5 = (\boldsymbol{J}_{u\Sigma}^b)^{-1}\cdot\boldsymbol{J}_n^c \tag{78c}$$

Let us underline, that in opposite to the classical partitioning [6], in the present case, the $\boldsymbol{B}_1$ and $\boldsymbol{B}_4$ matrices are different.

9. Considered model

Considered multibody system is composed of three planar bodies connected by a translational and two rotational joints (see fig. 6a). Lengths of the first and the second bodies equal $l_1 = l_2 = 0.2$ m. Length of the third body equals $l_3 = 0.3$ m. The fixing point between the reference and the first body (fig. 6b) is moved $x_1 = 0.41$ m left and $y_1 = 0.3$ m up from the beginning of the reference. The first body is made of a steal pipe. Its external diameter equals $D = 25$ mm, and the wall thickness equals $d = 3$ mm. Together with the electrical engine, gearbox and transmission (devoted to drive the second joint), its mass equals $m_1 = 1.72$ kg. Its moment of inertia equals $I_1 = 0.018$ kg·m^2. Position of the engine is selected according to the gravity balancing, i.e. the mass centre of the first body coincides with the joint axis. Mass of the second body (made of the similar pipe) is $m_2 = 0.45$ kg. Its inertia is $I_2 = 0.0025$ kg·m^2. Mass of the third body is $m_3 = 0.365$ kg. Its inertia is $I_3 = 0.00275$ kg·m^2. The mass centres of the second and the third body coincides with the geometrical centres of the bodies.

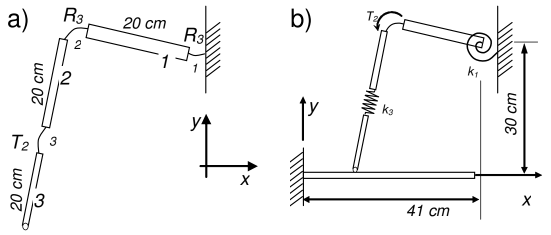

Figure 6: The multibody model: elements of the multibody system (a); the beam and the joint elasticity (b)

To drive the model, damping and stiffness are introduced in the first and the third joint. For the first joint, stiffness equals $k_1 = 10$ N·m/rad, and the damping is $c_1 = 0.1$ N·m·s/rad. For the third joint, stiffness equals $k_1 = 80$ N·m/rad, and the damping is $c_1 = 0.1$ N·m·s/rad. Finally, it is supposed that the second joint rotates with a constant speed ($\dot{q}_2 = 0.2$ rad/s).

The end-effector of the multibody system is in a contact with the cantilevered beam. The beam is *0.4* m long. Ten finite elements are introduced to model teh beam. The beam numerical data are: $a = 0.0015$ m (height); $b = 0.01$ (width); $\rho = 4.7 \cdot 10^3$ kg/m^3; (density), $E = 2.1 \cdot 10^{11}$ Pa (Young Modulus).

To confirm the model, numerical tests are performed. Selected configuration (obtained in the test) is presented in Fig. 7a. Relations between the friction coefficient and the driving torque (i.e. the Lagrange multiplier associated to the constraint enforcing the constant rotational speed) are presented in Fig. 7b.

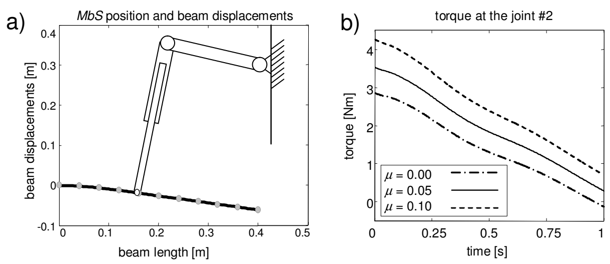

Figure 7: Numerical tests: the structure position at $t = 0.6$s (a); driving torque at joint #2 (b)

10. Summary and conclusions

Referring to the practical applications, the sliding contacts between the multibody systems and the deformable continues systems are essential in a significant number of cases. It is not a straightforward problem, as structurally different systems have to be joined by some common constraint equation. Additional complications arise when a slip friction is considered. In the case, the applied friction forces depend explicitly on Lagrange multipliers, i.e. are functions of the system dynamics.

The paper confirms that the required constraint equations can be formulated to model the contact in the finite element normal direction. As the introduced friction forces are proportional to the Lagrange multipliers, the generalized forces based on the friction forces can be linearly combined with the generalized forces based on the Lagrange multipliers. Thus, with the frictional sliding contact is modelled in the tangent direction, the dependent coordinates and the Lagrange multipliers can be eliminated, but a modified version of the coordinate partitioning is necessary. Presented relations confirm that the required modification is possible.

The proposed numerical algorithm is verified on a set of numerical calculations. A model of a pantograph connected with a cantilevered beam is proposed. The obtained results confirm numerical attractiveness of the proposed algorithm.

References

[1] Adaci, M., Terumichi, Y., Suda, Y. and Sogabe, K., Coupled motion between wheel and an irregular track for high speed trains. *Proceedings of the ECCOMAS Thematic Conference in Multibody Dynamics*, Politecnico di Milano, Milan, Italy, June 25-28, 2007.

[2] Allotta B., Pugi L., Bartolini F., Design and development of a railway pantograph with a wire-pulley transmission system. *Proceedings of the ECCOMAS Thematic Conference in Multibody Dynamics*, Politecnico di Milano, Milan, Italy, June 25-28, 2007.

[3] Ambrosio, J., Pombo, J., Rauter, F. and Pereira, M., A memory based communication for the co-simulation of multibody and finite element codes for the pantograph-catenary interaction simulation. *Proceedings of the ECCOMAS Thematic Conference in Multibody Dynamics*, Politecnico di Milano, Milan, Italy, June 25-28, 2007.

[4] Fisette P., Lipinski K., Samin J.C., Symbolic Modelling for the Simulation, Control and Optimisation of Multibody Systems, *Advances in Multibody Systems and Mechatronics*, Technische Universität Gratz, Gratz, Austria, September, 139–174, 1999.

[5] Fisette P., Samin J.C., *Symbolic Modeling of Multibody System*. Kluwer Acad. Pub. 2003.

[6] Haug, E.J. and Yen, J., Generalized Coordinate Partitioning Methods for Numerical Integration of Differential-Algebraic Equations of Dynamics, *NATO ASI Series*, *Vol. F69, Real-Time Integration Methods for Mechanical System Simulation*, Springer-Verleg Berlin, 1990.

[7] Lipiński, K.: Multibody system in a contact with a model composed of finite elements, *Proceedings of the ECCOMAS Thematic Conference in Multibody Dynamics*, Politechnika Warszawska, Warszawa, 29 czerwca-2 lipca, s.[1-17], 2009.

[8] Lipiński K.: Constraint equations between a multibody system and a model composed of finite elements (in Polish), *Modelowanie Inżynierskie*, 8 (39), pp. 127-134, 2010.

[9] Gawroński, W., Kruszewski, J., Ostachowicz, W., Tarnowski J. and Wittbrodt E., *Rigid finite elements method in dynamics of constructions* (in Polish), Arkady, Warszawa, 1984.

[10] Zienkiewicz, O.C. and Taylor, R.L., *The Finite Element Method*, *Vol. 1*: *The Basis*, fifth ed., Butterworth-Heinemann, Oxford, 2000.

[11] Frączek J., Wojtyra M., *Kinematyka układów wieloczłonowych, metody obliczeniowe*, WNT, Warszawa, 2008